Effect of Egg White Protein and Water Content on the Stabilization Mechanisms of Natural Rubber Latex Foams Obtained from Microwave Radiation

Clara Amezúa-Arranz, Leandra Oliveira Salmazo, Alberto López-Gil, and Miguel-Ángel Rodríguez-Pérez*

The global plastic consumption, as one of the paramount concerns of our society, opens new paths of investigation in green materials. This study presents contribution to the field with the obtention of natural rubber latex foams (NRLF using egg white powder (EW) as the biostabilizing agent. The route followed to develop these samples is based on a two-step process, a previous aeration, followed by microwave dehydration. This synthesis route is greener and ecofriendlier than conventional ones due to the use of bio-based bulk materials, the utilization of microwave radiation which reduces the energy consumption in comparison with conventional heating methods, and the elimination of the vulcanization process typically used when producing latex foams. Herein, a deep study of the effect of EW on NRLF obtained at three water content levels (i.e., 40, 70, 90 phr) is carried out. The density and cellular structure parameters are measured for the formulations of liquid and solid foams to comprehend the stabilization mechanisms due to the presence of the EW and the effect of water content. It has been possible to produce open-cell natural rubber latex foams with densities as low as 53 kg m^{-3} and cell sizes as low as 114 μm.

1. Introduction

Polymer foams are dispersions of gas in a continuous polymer phase.[1] Foamed polymer materials display a vast range of advantageous properties as low densities, good heat and sound insulation, high specific stiffness and strength, and buoyancy, among others.[2] Due to their high-quality properties, the global market of foamed polymer products is continuously increasing. It was valued at USD 128.0 billion dollar in 2022 and it is expected to reach 170.1 in 2030.[3] The complex properties of these products are driven by their density and cellular structure with parameters such as cell size, cell size distribution, anisotropy ratio, etc. To obtain their particular cellular structure, there exist a vast number of foaming procedures such as gas dissolution foaming, extrusion foaming, or reactive foaming to name a few. In some cases, such as polyurethane or latex foams, it is necessary to start from a liquid foam which acts as a precursor of the solid foam product.[2] In these cases, a deep understanding of the stability of the liquid foams to control the final solid sample is required.[1]

The main degeneration mechanisms that must be controlled in liquid foams are coarsening, coalescence, evaporation, and drainage.[1] Drainage is of particular importance in liquid foams because it can be affected by the effect of the gravity which provokes the liquid flowing from the top to the bottom of the foam (macroscopic drainage).[4–7] There could be also microscopic drainage, that is, the liquid flowing through the struts of the foam.[8] Both types of drainages may occur simultaneously in a liquid foam and if nothing is done to prevent them, they may cause cell degeneration and finally the collapse of the foam.

The conventional method used to avoid or delay the degeneration mechanisms in foams produced from liquids, especially drainage, is, on the one hand, the use of surfactants to stabilize the bubbles when the foam is still liquid. These surfactants are typically amphiphilic molecules that arrange at the interphase air/water delaying drainage and enable bubble maintenance and in consequence, foam formation. For instance, surfactants based on silicones[9,10] are used generally in the production of PU foams and surfactants based on potassium oleate[11,12] are used in the production of latex foams. On the other hand, curing agents such as sulfur[13] are used to crosslink the polymeric matrix in the cell walls and struts, increasing its viscosity and stabilizing the cellular structure of the final solid foam. However, the use of these additives makes the formulations to produce these foams very complex and the final solid foam not easily recyclable due to the high crosslinking degree of

C. Amezúa-Arranz, L. O. Salmazo, M.-Á. Rodríguez-Pérez
Cellular Materials Laboratory (CellMat)
Condensed Matter Physics Department
Faculty of Science
University of Valladolid
Campus Miguel Delibes, Paseo de Belén 7, 47011 Valladolid, Spain
E-mail: clara.amezua@uva.es

L. O. Salmazo, M.-Á. Rodríguez-Pérez
BioEcoUVA Research Institute on Bioeconomy
University of Valladolid
47011 Valladolid, Spain

A. López-Gil
CellMat Technologies S.L.
Paseo de Belén 9A, 47011 Valladolid, Spain

the polymeric matrix. Thus, one of the main industrial and academical challenges in the production of these foams is to find new sustainable alternatives for the additives used to stabilize liquid foams which may promote the development of new bio-based foams able promote circularity and better end-of-life options for foamed products.

Proteins are the most widespread surfactants in edible products.[14] Particularly, egg white powder is one of the most desirable proteinaceous surfactants used in the food sector because of it excellent foaming, emulsifying, heat setting, bonding, and gelling properties.[15,16] On a weight basis, EW consists of ≈88% water and 12% of solid matter whose 10% are proteins and the rest are minerals, sugars, and only a trace of fat. The paramount proteins present in the EW are ovalbumin (OVA, 54% w/w of EW protein), ovotransferrin (12% w/w), ovomucoid (11% w/w), lysozyme (3.5% w/w), and ovomucin (3.5% w/w).[17,18] EW proteins are amphiphilic molecules that in their native state are folded, forming aggregates in which the majority of the hydrophobic and hydrophilic regions are oriented toward the inside of their structure.[19] When gas is introduced into the liquid blend, protein molecules suffered a conformational change in their structure named surface denaturalization. This process is driven by the unfolding of the protein aggregates and the reorientation of their hydrophobic regions toward the gas phase forming cohesive viscoelastic films via large intermolecular interaction which enables aeration and promotes liquid foam stabilization.[20–22] The exceptional foaming ability of the egg white is connected to the great interaction between the various constituent proteins.[21] Moreover, proteins also denature while they are heated,[15] losing their initial conformation which led to intermolecular interaction creating a 3D gel network in which water molecules are entrapped, enhancing stability of the final dried sample. The gelling ability of EW proteins and the characteristics of the resulting gels are usually affected by protein concentration, the characteristics of the aqueous medium, and processing conditions.[19,21] These properties and change of state of the protein molecules in the presence of air bubbles and during heating could be used to produce stable foams from natural liquid latex without synthetic surfactants or crosslinkers.

Natural rubber latex (NRL) is a stable colloid dispersion that contains different isomers of polyisoprene and diverse proteins in an aqueous medium.[23] NRL is a green nature product whose paramount source is the specie of tree *Hevea brasiliensis*.[24] It is normally processed into high-ammonia NRL (HA-NRL) for its preservation and stabilization.[24,25] Its great strength, flexibility, and elasticity turn latex into a very attractive material for medical and industrial applications.[26] Also, it is an important material to produce low-density flexible foams for the cushioning sector and other applications because of their open-cell structure and resilience characteristics.[27] The conventional routes to obtain natural rubber latex foams (NRLF) are Dunlop and Talalay methods. According to the Dunlop process, the samples are obtained from a two-steps process based on whipping the initial liquid compound to be subsequently heated to finally produce the stable solid sample.[26,28] Due to its simplicity, reliability, and cost effectivity, the Dunlop method is commonly used to manufacture NRLF.[29] Talalay process is also used in the foam industry to obtain softer NRLF with better flexibility and mechanical properties.[30] Despite that, Talalay is more expensive and complex because it requires vacuum and a freezing system to stabilize the sample.[31] In both processes the liquid foam is stabilized by crosslinking agents such as sulfur and using surface heating methods for dehydration and curing, which require high energy consumptions and promote a heterogeneous heating of the liquid foam. In addition, the use of crosslinking agents results in a crosslinked material at the end of the process, which makes very difficult its recycling after use. This usually leads to cellular degeneration and in the end, to heterogeneous cellular structures. Some attempts have been made in literature to improve the structure of these foams. For instance, Sirikulchaikij et al.[28,30] prepared latex foams via the Dunlop method using bubbling technology to obtain foams with lower densities, spherical and interconnected cells, and crack-free structure, typical foam network obtained by the Talalay process. Their results showed the relation between these parameters with the increment of the air flow rate: density is reduced, cell size increases, and compression testing is enhanced. Other works are focused on improving structure and properties using more sustainable approaches, for instance, using electron beam irradiation,[32] ultrasonic irradiation,[31] replacing the normal vulcanization accelerator with a more sustainable complex,[33] or introducing fillers as reinforcement such as silver nanoparticles, egg shell powder, chitin, cellulose or bamboo and kenaf fibers.[23,25,29,34–39] For instance, Bashir et al.[23] improves the mechanical properties of their samples introducing egg shell powder, Phomrak et al.[29] obtained low-density samples with elevated porosity and interconnected cells and also enhanced the mechanical properties of the resulting foams by adding micro and nanofibers of cellulose, Mam et al.[35] developed NRLF with density of $700 \, \text{kg m}^{-3}$ available for cushioning applications with antibacterial properties due to the effect of silver nanoparticles, and Kudori et al.[38,39] improved the value of tensile modulus at 100% elongation of NRLF developed by Dunlop method adding kenaf core and bast fibers in the samples. Furthermore, NRLF has not only applications in the comfort sector, there are also innovative researches such as the use of recycle scraps from NRL for supercapacitor applications[40] or the fabrication of conductive polymer composites based on NRL, polydopamine, and silver nanoparticles to obtain piezoresistive sensors.[41]

Microwave radiation is a sustainable heating method which offers fast foam processing due to its centered heating generation from inside-out reducing energy consumption.[42] It has been used in literature to produce natural rubber foams[27,43] but from dry natural rubber and chemical blowing agents which are compounded in the solid state before foaming. However, as far as the author knows, the bibliography available about the use of microwave radiation to produce natural rubber foams from latex is very scarce.[44,45] In both articles, microwave irradiation is used to vulcanize the composite to obtain NRL foams through Dunlop method with cushioning performance for packaging applications. These studies illustrated the possibility of improving the sustainability of packaging cushion, reducing the energy consumption, and using sustainable bulk materials.

In this study, the use of egg white proteins as biostabilizing surfactants to replace typical crosslinkers used in the production of NRLFs is investigated. A two-step process based on liquid aeration by stirring, and a final dehydration process based on

microwave radiation to increase the dehydration speed and promote a more homogeneous heating, is used in this work. The use of different egg white protein concentrations and the use of latex with different initial water/solid contents are analyzed in detail. The liquid and solid foams are characterized to understand how the concentration of proteins and water influences the expansion/density and cellular structure of the foams and to understand the possible stabilization mechanisms occurring during the process.

2. Experimental Section

2.1. Materials

High-ammonia (HA) NRL including 60% dry rubber content and 40% water, employed as the polymer matrix, was supplied by LATEXA (Barcelona, Spain). Egg white powder used as stabilizer was purchased from Harrison Sport Nutrition S.L. (HNS, Granada, Spain). Tap water was used to dilute latex to different solid contents.

2.2. NRLF Production Process

The lab route to obtain these NRLF was based on a two-step process (**Figure 1**): an aeration to produce a liquid foam followed by dehydration using microwave radiation to produce the final solid and stable foam. First, 100 phr of latex with different water contents were blended with the corresponding amount of protein (egg white powder from 0 to 25 phr) in a whipping machine (MUM 50123 StartLine, Bosch) during ten minutes at full power (800 W). The liquid foamed sample was immediately transferred into a 60 mL syringe to fill a teflon mold and fill its cavity (diameter of 6.0 cm and height of 5.4 cm) maintaining this weight (10 g) in each experiment. The mold was used to control the growing of the foam and give it a final cylindrical shape. Teflon was used because it is transparent to microwave radiation.[46] Then, the mold was introduced into a microwave (SHARP R-939 with specifications: 40 L capacity, 2.45 GHz frequency, 900 W output power) in which the liquid foam was heated for 2 min at 900 W to finally obtain the solid samples. The time for microwave radiation was set in 2 min to ensure a complete dehydration of the foamed samples. It was important to remark that the time between aeration and dehydration was always maintained in 2 min to avoid air bubble losses and the collapse of the liquid foam.

For the preparation of high-water-content latex, the initial NRL (40% water) was diluted with the corresponding amount of tap water to obtain the water contents required before the blending process with proteins and aeration. Three foam series changing the water content present in the natural latex, 40 phr (undiluted original latex), 70 phr, and 90 phr, were studied. The formulations employed for the fabrication of NRLF are summarized in **Table 1**. The colored boxes were the foamed samples produced
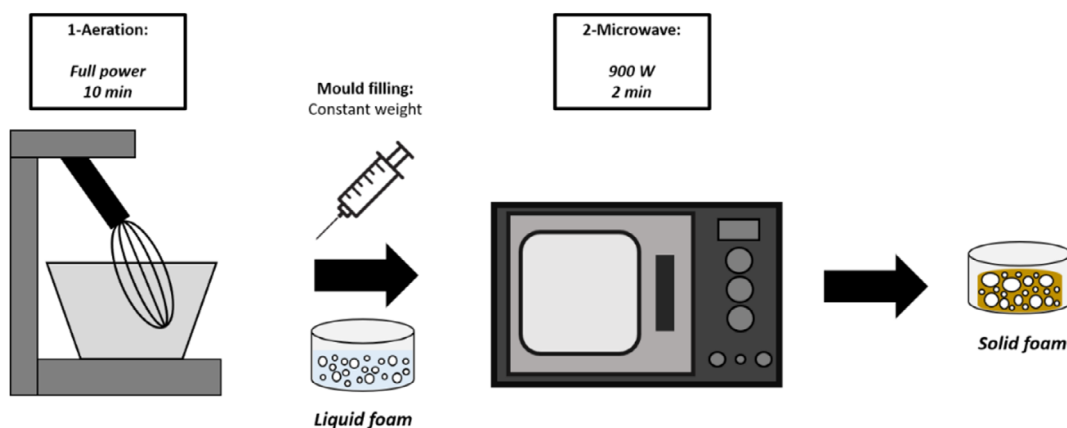

Figure 1. Lab route to obtain the NRLF developed through this work.

Table 1. Formulations of the NRLF developed in this work.

Type of latex [100 phr][a]	Total water [phr]/total solids [phr] in latex	Protein [phr][a]											
		0	0.5	1	2.5	5	7.5	10	12.5	15	17.5	20	25
40 WC (original non-diluted latex)	40/60	–	–	–	–	x	x	x	–	–	–	–	–
70 WC	70/30 (50 phr original latex + 50 phr tap water)	–	–	–	–	–	–	–	–	x	x	x	–
90 WC	90/10 (17 phr original latex + 83 phr tap water)	–	–	–	–	–	–	–	–	–	x	x	x

[a] Parts per hundred of NRL.

and characterized in this work. The green ones were liquid foams that resulted in a stable solid foam after dehydration, that is, the solid foam did not fully collapse. The red ones were unstable liquid foams with no protein added, which collapsed before the microwave process. Therefore, a solid foam was not produced from them. However, the liquid foam was characterized. The nonfilled boxes or white boxes corresponded to liquid foams which were neither characterized nor processed into the microwave oven for several reasons. In the case of the 40 WC series of foams (original nondiluted latex), concentrations of proteins above 10 phr led to very dense liquid foams (very low aeration) which were not tested for dehydration. This also occurred with the 70 WC foam filled with 25 phr protein. In the case of the diluted latex (70 and 90 WC Series), protein contents below 5 phr led to nonstable solid foams that fully collapsed during microwave heating.

The cross sections of the final stable foams after microwave heating are shown in **Figure 2**. Some of them presented an internal collapsed structure, that is, noticeably big cells can be observed with the naked eye, especially those produced with the lowest protein contents within each series of foams produced from different initial water contents. These were the 40 WC foams filled with 0, 0.5, 1, and 2.5 phr of protein. The 70 WC foams were filled with 5, 7.5, 10, and 12.5 phr of protein and the 90 WC foams filled with 5, 7.5, 10, 12.5, and 15 phr of proteins. Others were very homogeneous in the cross section and did not present internal cellular collapses. They were highlighted with an orange box in Figure 2. The cells in these foams present micrometric sizes which were evaluated and measured in this work using Scanning electron microscopy (SEM). These were the ones produced with the highest protein contents and are marked with an *x* in Table 1. These foams are the ones that are characterized in more detail in this work. Both the liquid and solid foams corresponding to these formulations were characterized by density and cellular structure measurements so that it is possible to assess the foaming mechanisms throughout the whole process.

3. Characterization Techniques

3.1. Density

Density measurements of liquid and solid foamed samples were performed by the geometric method, that is, by dividing the weight of each specimen between its corresponding volume (ASTM standard D1622-08). A precision balance (AT261 Mettler-Toledo balance) is used for the weight measurements. The liquid foam density was obtained by dividing the weight of the sample required to fill the teflon mold (prior to the dehydration process in the microwave) with the volume of the syringe displaced. For the density measurement of solid foams, small prismatic samples are extracted from the middle of the final dehydrated foams. At least three replicates per samples are measured. The volume of these samples is measured using a caliper and their weight using a precision balance.

The relative density of the foams (ρ_r), both liquids and solids, was in turn calculated as the ratio between the density of the final foam (ρ_f) and that of the corresponding liquid or solid material comprising the foams (ρ_s), as shown in Equation (1).

$$\rho_r = \frac{\rho_f}{\rho_s} \tag{1}$$

For liquid samples, ρ_f is the density of liquid foam after whipping and ρ_s is the density calculated by the rule of mixtures of the initial liquid blend based on latex at different water contents and the corresponding amount of protein. The density of the undiluted latex was experimentally measured as 982 kg m^{-3}, and in the case of the diluted latex, the calculations were done taking into account the correct proportions water/latex considering 1000 kg m^{-3} as water density. The density of egg white protein is 1230 kg m^{-3}.

For solid samples, ρ_f is the density of solid foam after the microwave dehydration process and ρ_s is the density of the solid matrix in the cell walls and struts of the foam, which is a blend of the dry natural rubber present in the latex and the protein added. The calculations were done by the rule of mixtures assuming the density of dry natural rubber as 930 kg m^{-3}.[32] Besides, for formulations with diluted latex, the amount of dry natural rubber must be recalculated considering the correct proportions of water/latex.

The volumetric expansion ratio (ER) of the foams was calculated inversely, that is, as the ratio between the solid or liquid density and the solid and liquids foam density, respectively (Equation (2)).
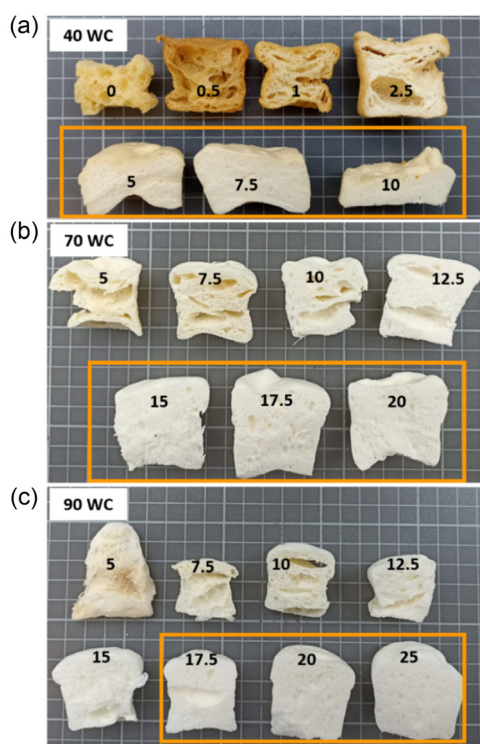
Figure 2. Solid NRLF series developed through this work at different water contents: a) 40 WC, b) 70 WC, and c) 90 WC.

$$\text{ER} = \frac{\rho_s}{\rho_f} \tag{2}$$

In addition, the porosity of the foamed samples (V_f), which represents the gas fraction in the material, was calculated using Equation (3).

$$V_f = 1 - \rho_r \tag{3}$$

3.2. Cellular Structure

The cellular structure of the liquid and solid foamed samples was evaluated by means of optical micrograph analyses for liquid foams, which were taken by a polarized light optical microscope (DM2500 M, Leica) with a digital camera (EC3, Leica) and for solid foams by a scanning electron microscope (FlexSEM 1000 VP-SEM, Hitachi). For liquid foams, optical microscopy images were taken 2 min after the aeration process in order to represent the moment just before microwave heating and 10 min after to study the temporal stability of the foams. For SEM micrographs, the foams were cut in their middle zone and the surface was coated with gold using a sputter coater (model SDC 005, Balzers Union, Liechtenstein) to finally visualize the growth plane (z) of the solid foam.

These micrographs were analyzed by an image analysis software ImageJ/FIJI[47] in which a binarization process was performed so as to isolate each bubble or cell from the rest, allowing the software to measure bubble or cellular structure parameters such as the bubble/cell size in 2D (ϕ) and anisotropy ratio (R).

For measuring the size of each bubble/cell, the software determined its center and then measured its length in eight different angles. Finally, it calculated the average diameter. The foam cell size is the average for all the cells considered in the image and the average cell size in 3D ($\phi3D$) was obtained by multiplying the 2D values by the correction factor 1.273.[47]

The homogeneity of the cellular structure was described by the normalized standard deviation (NSD) parameter, which represents the ratio between the standard deviation of the cell size distribution and the average cell size of each foam sample (Equation (4)).

$$NSD = \frac{SD}{\phi3D} \tag{4}$$

In addition, cell density (N_v) which is referred to the number of cells per unit volume of foam (cells cm^{-3}), was determined according to Equation (5), which takes into account the relative density (ρ_r) previously described and the cell size in 3D ($\phi3D$).[47]

$$N_v = \frac{6(1 - \rho_r)}{\pi(\phi_{3D})^3} \tag{5}$$

3.3. Thermogravimetric Analysis (TGA)

Thermogravimetric analysis (TGA) measurements were conducted on the solid foams under nitrogen atmosphere using a Mettler Toledo TGA/SDTA 851. In the experiment, a sample of the solid foams ($\approx$10 mg) was placed in an aluminum pan and was heated from 50 to 850 °C at 20 °C min^{-1}.

3.4. Dehydration of Solid Samples

To quantify the water loss after microwave, the percent of dehydration of the solid samples was measured using Equation (6).

$$\% \text{ Dehydration} = \left[\frac{W_{l.f} - W_{s.f}}{W_{l.f}}\right] \times 100 \tag{6}$$

where $W_{l.f}$ is the weight of the liquid foam before microwave heating and $W_{s.f}$ is the weight of the solid foam after microwave.

This value (% dehydration in the process) is compared with the water content of the initial blend latex or diluted latex with egg white proteins before aeration. The parts of water are the sum of the phr of tap water introduced in the case of diluted samples added to the amount of water present in the latex (40% of the initial parts of latex). These are the values of water content used to name the samples through the text (40, 70, and 90; see Table 1). Finally, to calculate the percent in weight of water content, the phr of water previously obtained with respect to the total parts of the mixture (phr water content + phr latex solids + phr egg white protein) must be considered.

3.5. FTIR Spectroscopy

The Fourier-Transform Infrared (FTIR) spectra were recorder on a Bruker Tensor 27 spectrometer using the ATR mode over the wavenumber range of 400–4000 cm^{-1} at 25 °C. The resolution of the device was 4 cm^{-1}, and air was scanned as the background of each sample. Each measurement was a superposition of 32 scans.

3.6. Mechanical Tests

Compression tests were performed by a universal testing machine (Instron model 5.500R6025) according to the standard ASTM D1621-00[48] at room conditions 23 ± 2 °C and 50 ± 10% of relative humidity, as indicated by ISO 291:2005.[49] The displacement rate was [height/10] mm/min and a load cell of $\approx$1 kN was used.

The elastic modulus (E) was calculated from the slope of the linear region of the compression curves.

4. Results and Discussions

Results and discussion is split up into two sections. First, the results and discussion, corresponding to the liquid foams, is the first step in the foaming process and second, the results and discussion corresponding to the solid foams is the second step in the foaming process.

4.1. Liquid Foams

The first step of the process to produce stable latex foams using proteins is the aeration step, in which the liquid latex together with egg white proteins are stirred and air becomes entrapped in the form of bubbles producing a liquid foam. An initial characterization of the liquid foams (NRLF) was carried out in order to better comprehend the events during aeration process and

**ADVANCED
SCIENCE NEWS**
www.advancedsciencenews.com

**ADVANCED
ENGINEERING
MATERIALS**
www.aem-journal.com

the role that egg white proteins play in this step of the process. The density values of the liquid foams whose formulations were described in Table 1 are shown in **Figure 3**; the labels marked in black are the formulations which led to stable solid foams (orange boxes in Figure 2 and boxes filled with an *x* in Table 1), which are also characterized by optical microscopy and image analysis.

Several results and tendencies can be observed in the graph of Figure 3. Firstly, at 0 phr protein content, the density of 40 and 70 WC liquid foams is very similar ($\approx$230 kg m^{-3}). The value of the foam with 90 WC could not be measured because the liquid foam was not stable enough and collapsed before the measurement. Therefore, the difference in water content in the foams without proteins (0 phr proteins) does not seem to vary the level of aeration or the amount of air entrapped into the foam.

Second, the addition of egg white proteins to the three different latex systems with different water contents resulted in different density evolutions with the increment of the protein content. In the 40 WC series (original nondiluted latex), the increment of the protein content led to an abrupt increment on the density. Contents of protein around 10 phr led to very dense liquid foam samples (400–450 kg m^{-3}). The tendency is different for the latex with higher water contents (70 and 90 WC). At low protein contents (below 10 phr), the density decreases and even a minimum in density at 7.5 phr protein content is detected in both systems. This is what would be expected considering the role of egg white proteins as surfactant and the stabilization mechanism by which they arranged themselves at the air–water interphase. They should allow the entrapment of more air bubbles and density reductions. In addition, this is also what has been observed in previous works where egg white proteins were used as surfactants but in different liquid media.[50,51] However, from 10 phr content, the density increases with the addition of more proteins, but this increment is not as abrupt as the one detected in the 40 WC foams. The explanation for this density increment detected in the three systems could reside in the high values of solids, which are present in the latex even at high water contents, creating an initial blend with high viscosity, which will

reduce its aeration capacity and the ability to entrap air bubbles. When more proteins are added, in the case of 70 and 90 WC latex above 10 phr content, the content of solids becomes higher and hence, the viscosity of the liquid blend. Besides, the whipping process may promote a surface denaturalization of the proteins, which may in turn promote the formation of protein aggregates and the creation of viscoelastic films between bubbles, which may increase further the viscosity of the liquid blend.[14,52]

Finally, the increment of the water content in the 70 and 90 WC latex in the presence of egg white proteins clearly promotes more aeration with respect to the 40 WC latex, diminishing the density of liquid foams even at very high EW contents. In fact, the lowest densities ($\approx$100–150 kg m^{-3}) are obtained for the formulations with 90 WC. The sharp reduction in the density of formulations with high water load could be related with the presence of less solids in the initial blend in comparison with the original nondiluted latex (40 WC), which will diminish the viscosity of this mixture increasing the space available to entrap air.

Before dehydration, the liquid foams and their internal bubble structure are observed by optical microscopy for 2 min (**Figure 4**) after aeration, which is the time set to introduce them into the microwave oven for dehydration, and are analyzed by image analysis and their structural parameters are collected in **Table 2**. The liquid foams used in this study are those leading to stable solid foams with no internal structural collapse, according to Table 1 and Figure 2.

A qualitative analysis of the micrographs allows to observe a higher number of bubbles or higher aeration level in the 70 and 90 WC foams, which is linked to the lower densities measured in these foams (Figure 3). The bubbles entrapped in these high-water liquid foams are also bigger or at least more heterogeneous
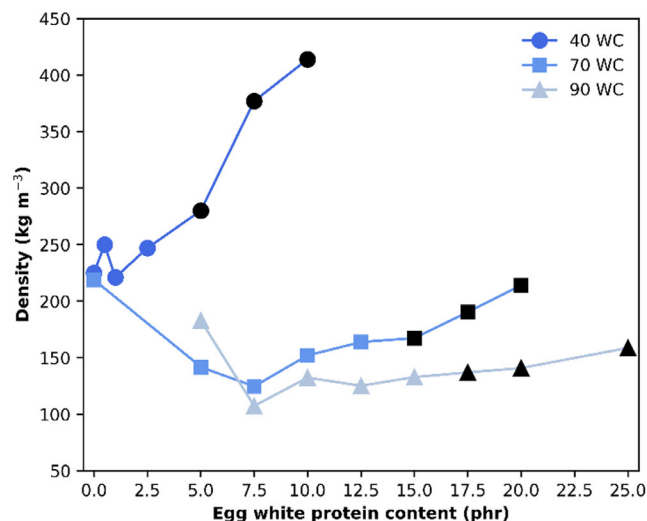
Figure 3. Density of liquid foams.
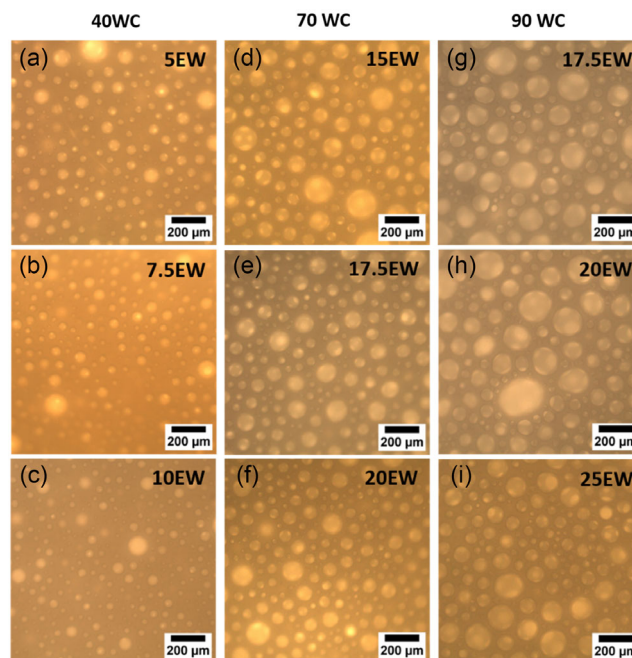
Figure 4. Optical microscopy images of a) 40WC-5EW, b) 40WC-7.5EW, c) 40WC-10EW, d) 70WC-15EW, e) 70WC-17.5EW, f) 70WC-20EW, g) 90WC-17.5EW, h) 90WC-20EW, and i) 90WC-25EW 2 min after aeration.

Table 2. Density and average structural parameters of liquid foams formulations which led to stable solid foams measured 2 min after aeration.

Formulation [phr WC-phr EW]	ρ [kg m^{-3}]	ρ_r	Φ_{3D} [µm]	NSD	R	$N_v \times 10^6$ [cells cm^{-3}]
40WC-5EW	280	0.281	56	0.48	0.99	7.70
40WC-7.5EW	377	0.376	51	0.50	0.98	8.87
40WC-10EW	414	0.410	40	0.54	1.01	17.56
70WC-15EW	167	0.162	73	0.56	1.00	4.06
70WC-17.5EW	190	0.184	61	0.56	0.98	6.94
70WC-20EW	214	0.206	53	0.56	1.02	10.26
90WC-17.5EW	137	0.132	77	0.72	0.98	3.69
90WC-20EW	141	0.135	65	0.79	1.01	6.11
90WC-25EW	159	0.151	64	0.63	0.99	6.22

bubble size distributions are observed. There do not seem to be clear differences with the protein contents in the high-water systems analyzed (70 and 90 WC). However, in the original latex (40 WC), a clear reduction in aeration, or a reduction in the number of bubbles, is observed with the increment of protein content, which is also linked to the abrupt density increment measured in these foams (Figure 3).

The bubble size distributions obtained by image analysis and shown in **Figure 5** confirm the previous qualitative analysis. The foams with higher water contents present broader bubble size distributions and they also appear to be more asymmetric. Bubbles with sizes lower than 50 µm and around 200 µm are present in the foams. On the contrary, the bubble size distributions of the liquid foams produced from the nondiluted latex (40 WC) are narrower and appear to be less asymmetric and closer to Gaussian distribution. The density in these foams is higher which may have promoted less degeneration and less heterogeneity in the bubble size distribution.

The main average gas-phase parameters linked to the bubbles formed in the liquid foams, together with the correspondent density (ρ) and relative density (ρ_r) values, are collected in Table 2.

On the one hand, formulations produced from the 40 WC latex, which present the highest relative densities, have cellular structures characterized for having bubble size 3D ranging from 0 to 200 µm, with average bubble size around 50 µm, the minimum values obtained. On the other hand, as water content increases, histogram bars shift to the right, that is, the number of bubbles with higher sizes grow. The average bubble size increases as well in comparison with the values achieved by 40 WC formulations. As a consequence, the bubble density values are reduced accordingly with the increment of the water content. Besides, the rather inhomogeneous cellular structure is also supported by the values of the NSD coefficient, in all cases
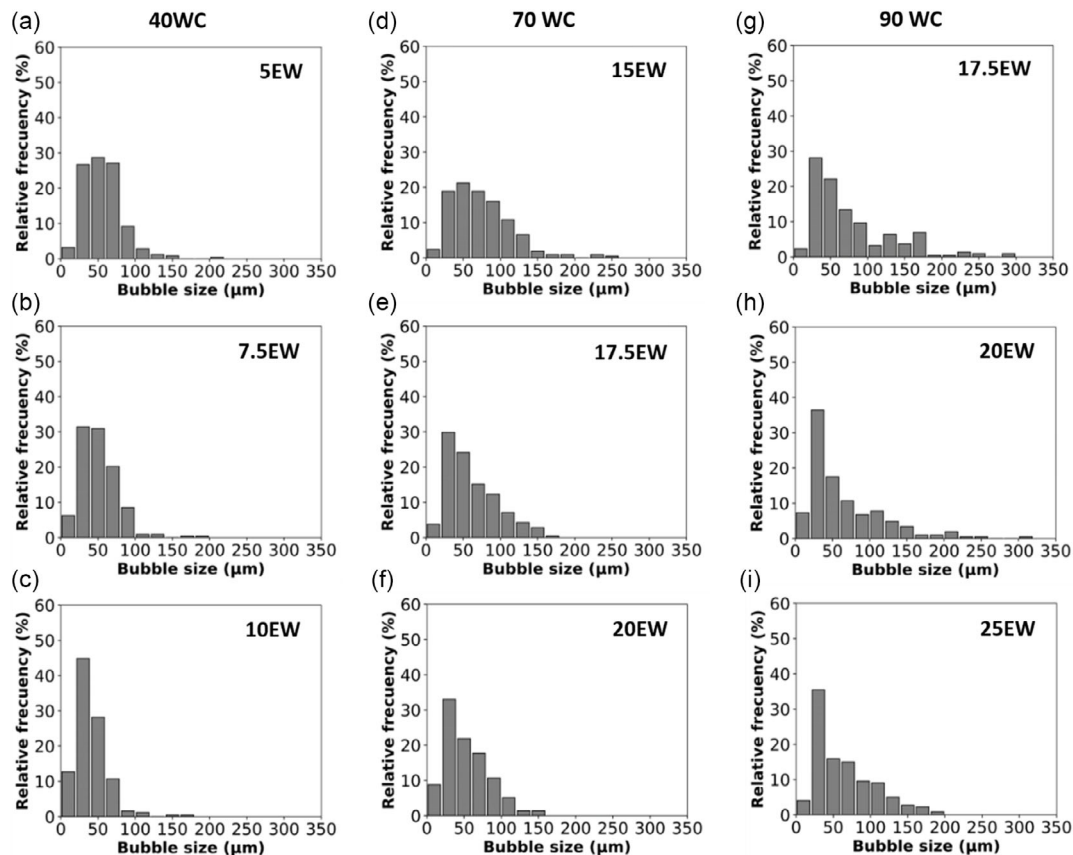
Figure 5. Bubble size distributions of a) 40WC-5EW, b) 40WC-7.5EW, c) 40WC-10EW, d) 70WC-15EW, e) 70WC-17.5EW, f) 70WC-20EW, g) 90WC-17.5EW, h) 90WC-20EW, and i) 90WC-25EW 2 min after aeration.

**ADVANCED
SCIENCE NEWS**

www.advancedsciencenews.com

**ADVANCED
ENGINEERING
MATERIALS**

www.aem-journal.com

around or even higher than 0.5, which, added to the histograms' distributions, confirms the heterogeneity of the foams. Qualitatively, microscopy images exhibit a vast range of bubble sizes in all samples but the bubble size distribution heterogeneity increases (higher NSD values) as the water content increases. Regarding the anisotropy ratio, these values are around 1 for all the formulations which are related to the spherical shape of the bubbles of liquid foams. In the three series of foams produced from different water contents, the increment of the protein content promotes a slight reduction of the bubble size and increment of the bubble density. In Figure S2, Supporting Information, a more detailed analysis of the evolution of the bubble size with the protein content for the 40 WC foams is included, in which an increment of the protein content promoted a reduction of the bubble size as well. Therefore, this trend is maintained at higher water contents. A bubble size reduction may promote stability to the liquid foam since these bubbles may be less prone to degeneration mechanisms.

The time stability of the liquid foams is another important aspect which is worth analyzing in more detail. Liquid foams are unstable systems in which drainage and coalescence could occur simultaneously, leading to the disappearance of bubbles through time, and this could be accelerated in the microwave process due to the rapid heating of the liquid. Therefore, a study of the temporal stability of those liquid foams leading to stable solid foams with no internal structural collapse is also carried out because it could be important to understand what occurs before and during the heating stage. This is done by comparing micrographs taken in liquid foams 2 min after aeration (when the liquid foam is put into the microwave oven for dehydration) and 10 min later (see **Figure 6**).

The qualitative observations that can be extracted from this figure are that EW proteins promote time stability because the liquid foams produced with high protein quantities (above 10 phr) seem to be still highly aerated 10 min after aeration. The number of bubbles in these foams is still high after this time. This stability is especially critical in the high-water-content foams

(70 and 90 WC) in which less solids are present and are more prone to drainage and degeneration mechanisms. However, the higher contents of proteins used in these foams allow to promote time stability and the liquid foams do not seem to lose aeration, although a tendency to increase the heterogeneity of the bubble size distribution is observed. Bigger bubbles are formed which are likely due to coarsening mechanisms. Furthermore, foams with an elevated content of protein are denser and more stable due to the enhancement of the thickness of the interfacial films.[51] In fact, some previous studies on the effect of different types of proteins in food foams and the evolution of the drainage of EW protein foams confirm this behavior.[14,52] These studies prove that the foam stability increases and the drainage becomes slow when protein aggregates are present in the foams. On the other hand, formulations with low quantities of protein (5 and 7.5 phr) and low water contents (original latex. 40 WC) present clear bubble losses. However, this reduction of the time stability in these two foams does not avoid the formation of a stable solid foam with no internal collapsed structure after dehydration in the microwave oven. This could be due to the high amount of solid present in the original latex, which counteracts the lower amount of proteins used in these foams and helps to promote stability during microwave dehydration. Moreover, these liquid foams are denser (Figure 3) so the cell degeneration process in the microwave oven may be less intense. (The liquid phase between bubbles is thicker.)

Figure S1 and S3 in Supporting Information provides more information about the time stability of liquid foams. A more complete study is carried out in the liquid foams produced from the original latex (40 WC) in which it is possible to observe how the time stability of the liquid foams is improved by increasing the content of proteins.

4.2. Solid Foams

The second step of the process is the production of solid foams by dehydrating the initial liquid foams obtained by aeration using
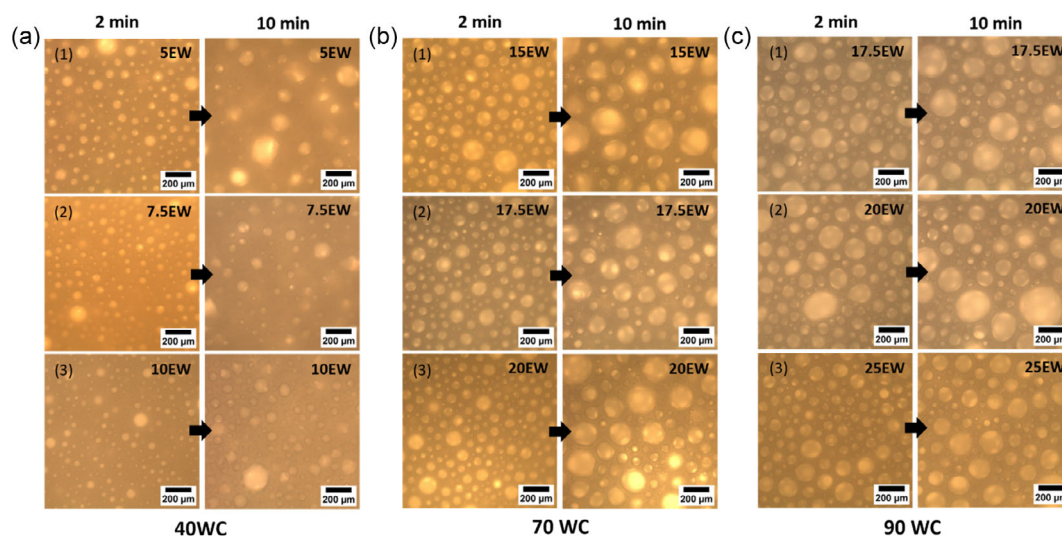
Figure 6. Optical microscopy images 2 and 10 min after aeration of a.1) 40WC-5EW, a.2) 40WC-7.5EW, a.3) 40WC-10EW, b.1) 70WC-15EW, b.2) 70WC-17.5EW, b.3) 70WC-20EW, c.1) 90WC-17.5EW, c.2) 90WC-20EW, and c.3) 90WC-25EW.

**ADVANCED
SCIENCE NEWS**

www.advancedsciencenews.com

**ADVANCED
ENGINEERING
MATERIALS**

www.aem-journal.com

microwave radiation. During this step, the liquid foam is quickly heated and water is evaporated, leading to the growth of the bubbles present in the liquid foam, due to the steam generated, and to the dehydration of the liquid lamella between bubbles, which becomes thinner as dehydration progresses. At the end, and as long as the thin polymeric phase between cells has enough stability, a solid foam is obtained with an internal cellular structure.

From now on, a detailed characterization of the stable foams (without internal collapse, Figure 2) obtained with each type of initial latex (40, 70, 90 WC) after microwave dehydration will be carried out. The formulations of these stable NRLF are the following: 40WC-5EW, 40WC-7.5EW, 40WC-10EW, 70WC-15EW, 70WC-17.5EW, 70WC-20EW, 90WC-17.5EW, 90WC-20EW, 90WC-25EW (the ones within the orange boxes in Figure 2).

First, it is important to know the dehydration levels of the solid foamed samples in order to determine whether the final sample is completely dried and therefore, stable. **Figure 7**a collects the theoretical water content and experimental dehydration values obtained following the procedure described in Section 3.4. Regarding both parameters, it can be concluded that the dehydration is completed after the process, as the two measurements achieve practically the same values for all the samples.

Figure 7b shows the TGA of the solid foam samples under evaluation. Two references have been included to better understand the thermograms: a solid foam just produced with latex and no egg white protein added (the same observed in Figure 2a) and an additional solid foam produced just with water (no latex) and egg white protein (100WC-20EW). These studies help to understand the different weight drops linked to egg white protein and to latex in the foams produced from both. In the foam produced just with latex (no stable), there is only one significant weight drop at 383.75 °C, which is linked to the thermal degradation of isoprene.[53] The content of residues left after the isoprene thermal degradation is scarce. In the foam produced just with egg white proteins, the main weight drop occurs at 312 °C, which is linked to the thermal degradation of egg white proteins,[51,54] in this case the amount of residues is much higher ($\approx$40%). This graph showed how there are no significant changes in the weight at 100 °C (water vaporization temperature), which means that most water is evaporated in the microwave process,
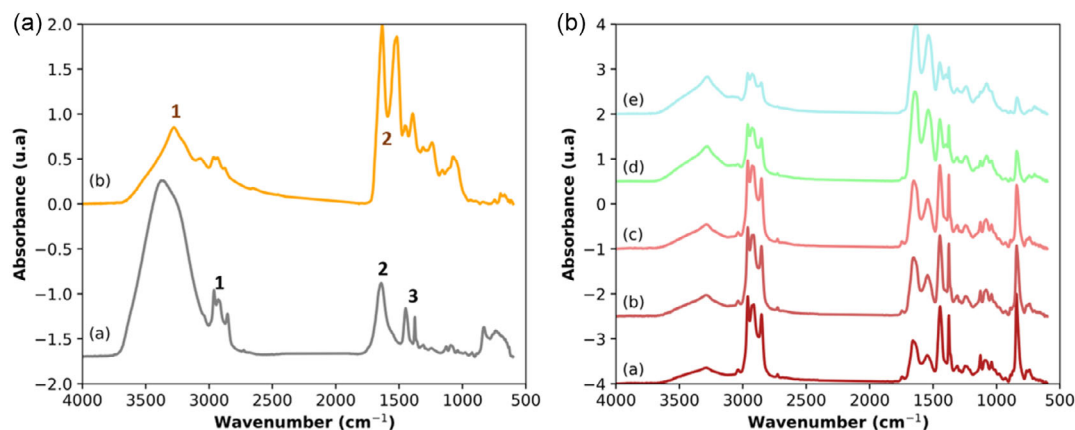
as already observed in the dehydration measurements (Figure 7a). The solid foams produced from latex and egg white proteins present in general two degradation steps, the first one at a lower temperature (around 315 °C) associated with the egg white protein thermal degradation and the second one at a higher temperature (around 380 °C) related to the thermal degradation of the solid components of the latex (isoprene and other constituents[25]). The solid foam with the minor water content (40 WC) has also lower protein content so the step associated with EW is barely inexistent, whereas their degradation step coincides totally with the degradation of the latex. Therefore, while water content increases and as well as the egg white protein, there appears the step of the protein that will become closer to the reference step when the amount of additive of the sample becomes higher. In addition, the second step of these samples is the same as the latex reference. Particularly, TGA thermograms of 70 and 90 WC formulations with high quantities of egg white present a huge amount of residues which may be related to the remnant of the protein after thermal degradation.[55,56] The solid matrix in the final solid foams is therefore a combination of egg white protein aggregates and natural rubber. The more egg white protein and the more diluted the initial latex is, the lower the thermal degradation of the foams since egg white proteins are less thermally stable.

FTIR was used to investigate possible modifications of the chemical structure of the raw materials in the formulations to produce foams. **Figure 8**a shows the FTIR spectra of the raw NRL and egg white powder.

For NRL (Figure 8a.*a*), the vibrational spectrum of pure NRL resembles the characteristic FTIR spectrum reported in the literature,[57,58] which mainly corresponds to that of the cis-isoprene structure, the main constituent of the NRL. The paramount bands are associated with the C–H stretching at 2960 cm^{-1}, the symmetric and asymmetric stretching of the CH$_3$ group at 2920 and 2855 cm^{-1} (region 1), and the symmetric and asymmetric bending of the same group at 1447 and 1376 cm^{-1} (region 3). The domains associated with the rest of constituents (regions 2 and 3) of the NRL are described by the amine in 3282 cm^{-1}, amide I in 1630 cm^{-1} and amide II in 1541 cm^{-1} bands for the proteins, and by the ester and carboxyl band around
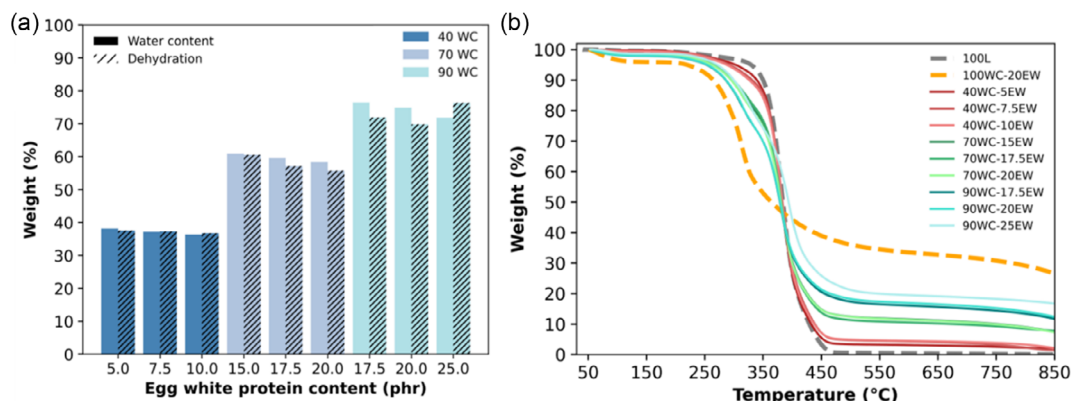
Figure 7. a) Graphic representation of theoretical water content and dehydration values of the stable formulations under study and b) TGA curves of the stable solid foams, foam obtained from 100 phr of undiluted latex and 0 phr EW (100 L) and foam obtained from 0 phr of latex and 20 phr of protein (100WC-20EW) used as reference to compare.

ADVANCED
SCIENCE NEWS
www.advancedsciencenews.com

ADVANCED
ENGINEERING
MATERIALS
www.aem-journal.com

Figure 8. a) FTIR spectra of (a) NRL and (b) egg white powder, and b) FTIR spectra of the following stable solid foams: (a) 40WC-5EW, (b) 40WC-7.5EW, (c) 40WC-10EW, (d) 70WC-20EW, and (e) 90WC-25EW.

$1700\,cm^{-1}$ for the phospholipids. For egg white protein, the main vibrational bands shown in Figure 8a.b are reported as well in the literature.[59,60] Broad bands in the range of $3600–3100\,cm^{-1}$ are related with O–H stretching, N–H stretching vibration at $3291\,cm^{-1}$ (region 1), stretching vibrations of the C=O bond are represented by the amide I region between 1700 and $1600\,cm^{-1}$, and the amide II region between 1600–1500 is related with bending vibrations of the N—H bond (region 2).

Figure 8b shows the FTIR spectra of different stable solid foams of NRLF under study. The formulations were selected to see differences in the spectra between stable solid foams at the same water content varying the amount of protein (40WC-5EW, 40WC-7.5EW, and 40WC-10EW), and stable solid foams with high protein content changing the amount of water (70WC-20EW and 90WC-25EW). Those spectra presented bands related with both NLR and EW raw materials. Regarding the samples at the same water content (Figure 8b.a,b,c), the bands belonging to the region 1 and 3 of the NRL spectrum (Figure 8a.a) appear with the same intensity for the three foams, whereas the bands included in the region 2 of the EW (Figure 8a.b) become more intense when the amount of protein of the formulation increases. Comparing the three water contents (Figure 8b.a,d,e), the intensity of the bands of the region 1 and 3 of the NRL decreases with the amount of water content, the peaks belonging to 90WC-25EW sample being the lowest. However, the intensity of the bands related with EW (region 2 of EW spectrum) increases.

The FTIR spectra obtained in this work do not show clear evidence neither of any important chemical modification in the initial raw materials, latex, or egg white, nor of the unfolding suffered by the proteins during the production of the foams. According to literature, the study of the unfolding of proteins requires a more detailed analysis of the amide I band frequencies $(1600–1700\,cm^{-1})$. In previous works where the effect of microwave heating on egg white was studied, it was proved that the order of proteins is modified by the microwave radiation, suggesting the unfolding of the proteins during heating treatment. This is what could also be happening in the foams produced in this work which helps to stabilize the structure.[61]

The density of the liquid foams and the correspondent stable solid foams without internal cellular collapse are compared in **Figure 9**a. A density ratio for both foams, liquid and solid, which is shown in Figure 9b., is calculated as the density of the solid foam is divided by the density of the liquid foam. This ratio indicates whether there has been a density increment or reduction in the microwave step. Ratios lower than 1 indicate a density reduction; therefore, a density reduction during the microwave dehydration step was detected. The sample suffered a mass reduction as the water of the liquid foam is evaporated through the microwave process.

In all the solid foams analyzed, regardless of the initial water content of latex, the density of the solid foam is much lower than the density of the initial liquid foam. This is confirmed in the density ratio parameter which is much lower than 1 for all the foams analyzed. This density reduction can be explained considering the quick dehydration and steam generation process that the foam undergoes during the microwave heating process. The loss of water from the liquid phase may promote the thinning of the liquid lamella between bubbles and at the same time, either the growing of the initial air bubbles present in the liquid foam by the steam pressure generated inside or the creation of new cells by nucleation in the dehydrated phase between them. Moreover, as explained previously, heating EW protein led to its denaturalization and gel formation.[18] Therefore, the viscosity of the liquid phase between bubbles increases because the proteins form a viscous gel which helps to stabilize the cellular structure and the foam until it gets fully dehydrated. Therefore, proteins are not only stabilizing the air bubbles in the liquid, but they are also stabilizing the solid while it is being dehydrated due to the formation of a more viscous gel. The tightness of the 3D gel network depends on the protein content.[19,21] The higher the amounts of EW, the tighter the network, which will promote stability to the final foam, although it seems that foamability is reduced. As observed in Figure 9a, the higher the protein content, the higher the density of the final solid foams (except for those produced from the most diluted latex, 90 WC). The obtention of low density and noncollapsed structures for formulations with high water loads could be related with the elevated contents
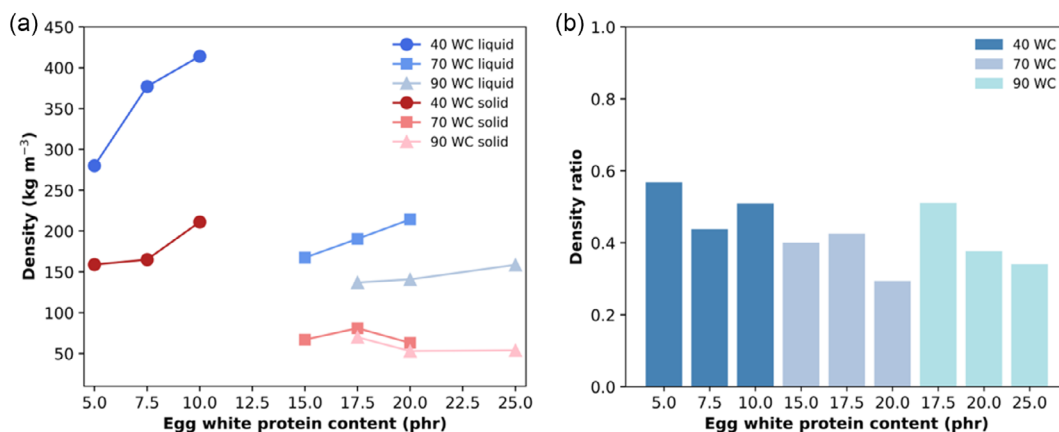
Figure 9. a) Density of stable liquid and solid foams developed in this investigation and b) density ratio of the stable formulations.

of protein used to obtain these samples, which enables the foam to retain most of the water steam generated through the microwave process and expand properly.

The trend followed by 40 WC solid foam series is the same as liquid foams, the density increases with the amount of egg white protein, achieving densities higher than $200 \, kg \, m^{-3}$. It seems that the level of aeration achieved in the initial liquid foam influences the final density of the solid foam. The more the air in the liquid foam, the lower the density in the solid foam. Therefore, the foams produced from the diluted latex (70 and 90 WC) which are the ones that aerate more (the density of the initial liquid foams is lower) are also the ones with the lowest solid foam densities, reaching values as low as $50 \, kg \, m^{-3}$.

The lowest density ratio values (Figure 9b) are obtained for the foams produced from 70 WC. This may mean that this is the combination of initial water content and protein content, which promotes more stability during the microwave dehydration process, since the density reduction obtained is higher.

The microstructure of the solid foams is also analyzed in detail. SEM micrographs and cell size distributions of the different stable solid foams are shown in **Figure 10** and **11**. The micrographs show partially open cellular structures in which many cells are interconnected by ruptures of different sizes in the cell walls. This partially interconnected structure may be formed during the dehydration step. The walls become thinner as drainage progresses and as the bubbles grow and at a certain point they break. Moreover, the structures are highly heterogeneous in terms of cell shape and size. Some foams present elongated cells (for instance 40WC-10EW), which may be formed due to the production of the foam inside a mold and the restriction of the expansion to one direction. In other cases, such as in foam 70WC.15EW cells are more spherical.
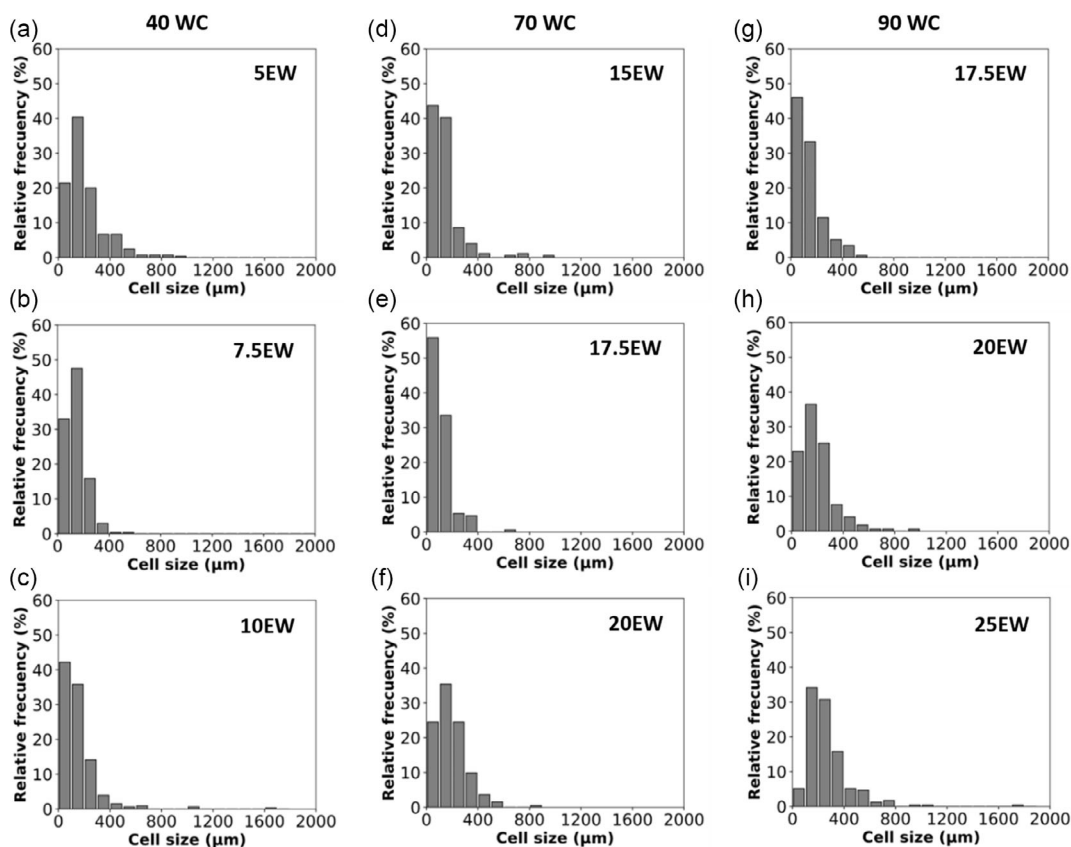
The cell size distributions (Figure 11) become broader than in the initial liquid foams. In the solid foams, cell with sizes lower than 50 µm and cells with sizes as high as 1 mm can be found. All the foams, regardless of the initial water content and the protein content present very heterogeneous cell size distributions and no clear differences are observed in this aspect.

The main average gas-phase parameters linked to the cells formed in the solid foams, together with the correspondent density (ρ) and relative density (ρ_r) values, are collected in **Table 3**.
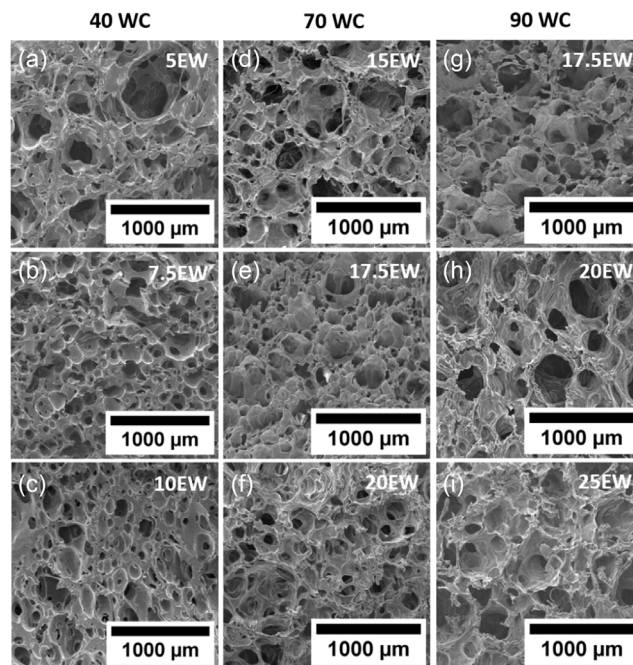
Figure 10. SEM micrographs of a) 40WC-5EW, b) 40WC-7.5EW, c) 40WC-10EW, d) 70WC-15EW, e) 70WC-17.5EW, f) 70WC-20EW, g) 90WC-17.5EW, h) 90WC-20EW, and i) 90WC-25EW.

Regarding the average cell size (Table 3), these foams present values in the range of 110–275 µm, lower than the ones obtained in other study for NRLFs produced by Dunlop method.[28] It seems that increasing the water content promotes cell degeneration and a cell size increment This is especially clear in foams 90WC-20EW and 90WC-25EW. This may be due to the lower density of foams produced with more diluted latex (70 and 90 WC). The cellular structure is less stable at low densities and tends to degenerate more, leading to bigger cells. Qualitatively, these samples present a heterogeneous structure justified by the values of NSD, which are in most cases higher than 0.5 and the shape of histograms which cover a huge interval of cell size values. In general, the foams exhibit anisotropy ratios

**ADVANCED
SCIENCE NEWS**

www.advancedsciencenews.com

**ADVANCED
ENGINEERING
MATERIALS**

www.aem-journal.com

Figure 11. Histogram distributions of a) 40WC-5EW, b) 40WC-7.5EW, c) 40WC-10EW, d) 70WC-15EW, e) 70WC-17.5EW, f) 70WC-20EW, g) 90WC-17.5EW, h) 90WC-20EW, and i) 90WC-25EW.

Table 3. Density and average structural parameters of stable solid foams formulations with 40, 70, and 90 phr water content.

| Formulation	ρ [kg m^{-3}]	ρ_r	Φ_{3D} [μm]	NSD	R	$N_v \times 10^5$ [cells cm^{-3}]
40WC-5EW	159	0.166	207	0.73	1.11	1.80
40WC-7.5EW	165	0.170	143	0.52	1.06	5.45
40WC-10EW	211	0.215	150	1.01	1.36	4.41
70WC-15EW	67	0.064	143	0.91	1.19	6.09
70WC-17.5EW	81	0.076	114	0.73	1.26	11.89
70WC-20EW	63	0.059	192	0.63	1.06	2.54
90WC-17.5EW	70	0.061	137	0.77	0.96	6.91
90WC-20EW	53	0.046	202	0.67	1.11	2.22
90WC-25EW	54	0.047	275	0.65	1.08	0.88

greater than one, indicating a slight degree of orientation through the growth direction, which may be because the liquid foam is dehydrated within a mold and expansion is restricted to one direction. Finally, in terms of cell density for solid foams, there are no dependencies between this parameter with the amount of protein or water content.

The cell size and cell density values of both liquid and solid foams are compared in **Figure 12**. It is possible to observe how in

general terms the cell size increases, and the cell density decreases during the microwave step, regardless of the water content of the latex being analyzed. It seems that the degree of variation is similar for the three types of latex. Moreover, the corresponding ratios of these magnitudes calculated as same as the density ratio (Figure 9b) are represented in the same Figure 12b,d. These ratios allow to observe the degree of cell size increment and cell density reduction, so it is possible to analyze the cellular structure stability of the foam during the microwave step. It is interesting to note that the foams produced from latex with higher water contents seem to be more stable since the cell size ratios are similar or even in some cases lower and the cell density ratios are higher. This is clearer in the 70 WC foams, which seem to be the more stable system in structural terms during the microwave step. The fact of using higher content of proteins in these foams and the fact of having more water, which may contribute to foaming in the microwave step, could be the reason why these foams are more stable during the microwave step.

Mechanical properties of some NRLF developed through this work are displayed in **Figure 13** and in Table S1 of Supporting Information. For the selection of the samples under study, the same criteria followed in the FTIR section are taken into account.

Density presents a huge influence on the mechanical properties of the NRLF chosen. The solid foams with the highest
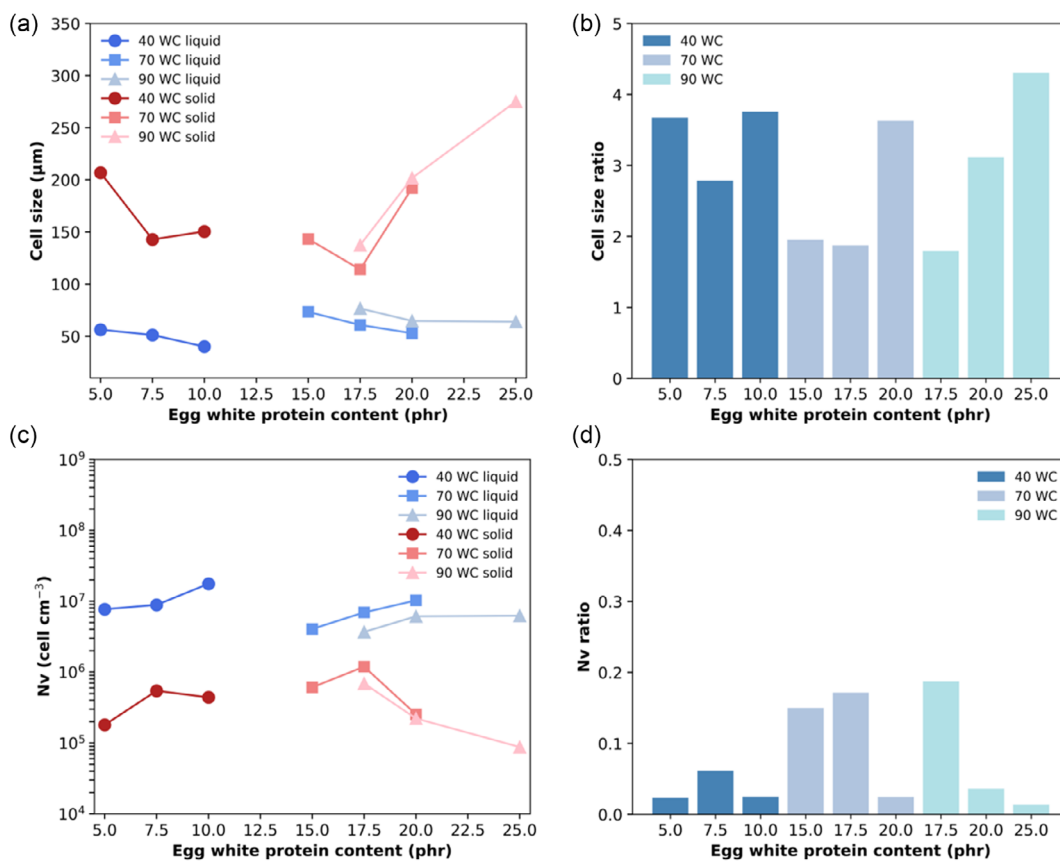
Figure 12. a) Cell size of stable liquid and solid foams developed in this investigation, b) cell size ratio of the stable formulations, c) cell density of stable liquid and solid foams developed in this investigation, and d) cell density ratio of the stable formulations.
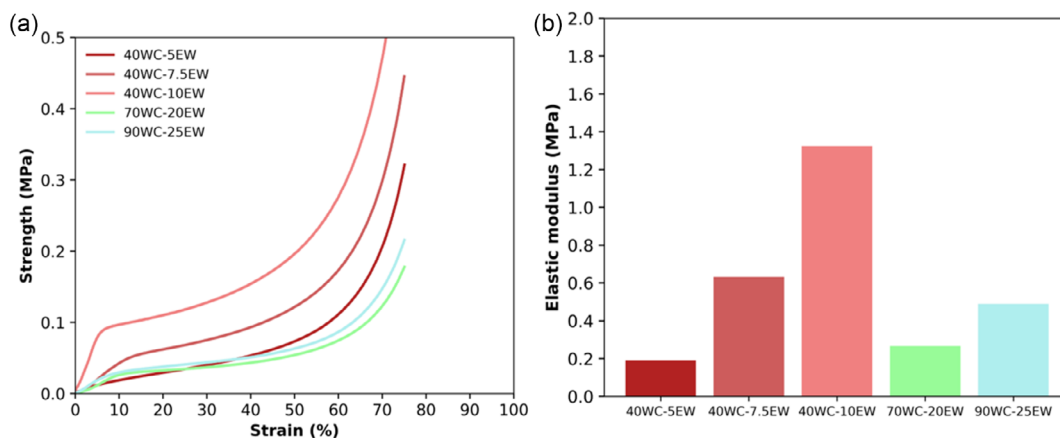
Figure 13. a) Stress–strain curves and b) elastic moduli for the solid NRLF under study.

densities (165 kg m^{-3} for 40-7.5EW and 211 kg m^{-3} for 40WC-10EW) require higher values of stress to perform the compression tests (Figure 13a), which led to an increment of the magnitude of their elastic modulus. Stress–strain curves show that the amount of protein seems to affect the mechanical strength of the foam as it is necessary to increase the stress applied to carry out the experiments (see the curves for 40WC-5EW, 40WC-7.5EW,

and 40WC-10EW in Figure 13a). Besides, the modulus value associated with those three formulations suffered a sharp increment (Figure 13b), reaching 1.32 MPa for 40WC-10EW. Increasing the water content promotes the obtention of less modulus value even for the samples with highest amounts of protein (70WC-20EW and 90WC-25EW). In addition, the trend followed by their stress–strain curves is similar to 40WC-5EW. From these

results, it can be concluded that the amount of solid contents present in the sample highly affects the mechanical properties of the foam.

5. Conclusion

Stable solid foams without internal structural collapse could be produced from noncured latex using egg white protein as the only stabilizing additive in the initial formulation. They are produced from a two-step process: liquid aeration and microwave dehydration. During the first step, proteins act as surfactants promoting aeration and time stability. In this liquid system, the increment of the protein content does not increase aeration. This may be due either to high solid content of latex, even when it is diluted, and to the possible formation of protein aggregates due to the stirring process. Both factors may increase the viscosity of the liquid and to prevent aeration. The dilution of latex helps to reduce the initial viscosity of latex and promote more aeration, but density still increases with the addition of high amounts of proteins (above 10 phr) although at a much lower extent than in the original latex. The time stability of the liquid foams increases with the addition of more protein.

In the second step, the quick dehydration of the liquid foams using microwave heating allows density reductions with respect to the liquid foams and a stabilization of the solid foams before collapsing. At high protein contents, the stability is very high, and the interior of the foams do not present internal collapses. For high water content latex, the content of proteins is needed to promote internal stability increase with respect to the original nondiluted latex. This good stability may arise from different factors, on the one hand, because of the higher liquid foam densities at high protein concentrations, and on the other hand, because proteins in the liquid phase may denature and aggregate during the heating process, creating a 3D gel network which leads to very sudden and high-viscosity increments stabilizing the cells in the foam.

These results prove that proteins may play two stabilizing roles in the production of bio latex foams: one as a surfactant providing time stability to the liquid foams and the other as stabilizing particles in the solid foams by increasing the viscosity of the matrix during foam expansion by steam generation. The more stable foams are the ones produced with 70 phr water content (a diluted latex) since these are the ones suffering from higher expansion increments and lower cell size increments during microwave heating. They are likely the ones presenting the right balance between initial solid contents and initial liquid foam density before the microwave foaming step. In this case, foams with densities as low as $63 \, \text{kg m}^{-3}$, and cell sizes as low as $114 \, \mu\text{m}$ and with an interconnected cellular structure, were obtained, which may be promising for applications where latex foams are typically used such as in cushioning.

Supporting Information

Supporting Information is available from the Wiley Online Library or from the author.

Conflict of Interest

The authors declare no conflict of interest.

Data Availability Statement

The data that support the findings of this study are available from the corresponding author upon reasonable request.

[1] E. Rio, W. Drenckhan, A. Salonen, D. Langevin, *Adv. Colloid Interface Sci.* **2014**, *205*, 74.

[2] A. van der Net, A. Gryson, M. Ranft, F. Elias, C. Stubenrauch, W. Drenckhan, *Colloids Surf., A* **2009**, *346*, 5.

[3] Polymer Foam Market Size, Share & Trends Analysis Report By Type (Polyurethane, Polystyrene, Polyolefin, Melamine, Phenolic, PVC), By Application, By Region, And Segment Forecasts, 2020–2030, https://www.grandviewresearch.com/industry-analysis/polymer-foam-market.

[4] P. M. Kruglyakov, S. I. Karakashev, A. V. Nguyen, N. G. Vilkova, *Curr. Opin. Colloid Interface Sci.* **2008**, *13*, 163.

[5] S. Jun, D. D. Pelot, A. L. Yarin, *Langmuir* **2012**, *28*, 5323.

[6] S. A. Koehler, S. Hilgenfeldt, H. A. Stone, *Langmuir* **2000**, *16*, 6327.

[7] T. N. Hunter, R. J. Pugh, G. V. Franks, G. J. Jameson, *Adv. Colloid Interface Sci.* **2008**, *137*, 57.

[8] S. A. Koehler, S. Hilgenfeldt, E. R. Weeks, H. A. Stone, *Phys. Rev. E* **2002**, *66*, 4.

[9] H. Lim, S. H. Kim, B. K. Kim, *Express Polym. Lett.* **2008**, *2*, 194.

[10] X. D. Zhang, C. W. Macosko, H. T. Davis, A. D. Nikolov, D. T. Wasan, *J. Colloid Interface Sci.* **1999**, *215*, 270.

[11] R. Roslim, M. Y. A. Hashim, P. T. Augurio, *J. Eng. Sci.* **2012**, *8*, 15.

[12] R. Ramli, A. B. Chai, S. Kamaruddin, J. H. Ho, F. R. Mohd. Rasdi, D. S. A. De Focatiis, *J. Rubber Res.* **2021**, *24*, 615.

[13] N. Kumkrong, P. Dittanet, P. Saeoui, S. Loykulnant, P. Prapainainar, *J. Polym. Res.* **2022**, *29*, https://doi.org/10.1007/s10965-022-03129-9.

[14] B. S. Murray, *Curr. Opin. Colloid Interface Sci.* **2020**, *50*, 101394.

[15] V. Lechevalier, R. Jeantet, A. Arhaliass, J. Legrand, F. Nau, *J. Food Eng.* **2007**, *83*, 404.

[16] X. Dong, Y. Q. Zhang, *J. Biomed. Mater. Res. Part B* **2021**, *109*, 1045.

[17] T. L. Parkinson, *J. Sci. Food Agric.* **1966**, *17*, 101.

[18] Y. Mine, *Trends Food Sci. Technol.* **1995**, *6*, 225.

[19] I. Rombouts, A. G. B. Wouters, M. A. Lambrecht, L. Uten, W. Van Den Bosch, S. A. R. Vercruysse, J. A. Delcour, *Innovative Food Sci. Emerg. Technol.* **2020**, *66*, 102484.

[20] J. R. Clarkson, Z. F. Cui, R. C. Darton, *J. Colloid Interface Sci.* **1999**, *215*, 333.

[21] L. Campbell, V. Raikos, S. R. Euston, *Nahrung - Food* **2003**, *47*, 369.

[22] A. Saint-Jalmes, M. L. Peugeot, H. Ferraz, D. Langevin, *Colloids Surf., A* **2005**, *263*, 219.

[23] A. S. M. Bashir, Y. Manusamy, T. L. Chew, H. Ismail, S. Ramasamy, *J. Vinyl Addit. Technol.* **2017**, *23*, 3.

[24] M. Singh, *J. Rubber Res.* **2018**, *21*, 119.

[25] N. Zhang, H. Cao, *Materials* **2020**, *13*, 1.

[26] A. Raveshtian, M. Fasihi, R. Norouzbeigi, S. Rasouli, *Thermochim. Acta* **2021**, *707*, 179108.

[27] Z. M. Ariff, L. O. Afolabi, L. O. Salmazo, M. A. Rodriguez-Perez, *J. Mater. Res. Technol.* **2020**, *9*, 9929.

[28] S. Sirikulchaikij, R. Kokoo, M. Khangkhamano, *Mater. Lett.* **2020**, *260*, 126916.

[29] S. Phomrak, A. Nimpaiboon, B. Z. Newby, M. Phisalaphong, *Polymers* **2020**, *12*, 1959.

[30] S. Sirikulchaikij, B. Nooklay, R. Kokoo, M. Khangkhamano, *Mater. Sci. Forum* **2019**, *962*, 96.

[31] B. Sukkaneewat, S. Utara, *Ultrason. Sonochem.* **2022**, *82*, 105873.

[32] L. O. Salmazo, A. Lopez-Gil, Z. M. Ariff, A. E. Job, M. A. Rodriguez-Perez, *Ind. Crops Prod.* **2016**, *89*, 339.

[33] W. Zhang, L. Lin, J. Guo, M. Wu, S. Park, H. Yao, S. H. Paek, G. Diao, Y. Piao, *Research* **2022**, *2022*, https://doi.org/10.34133/2022/9814638.

[34] S. Pinrat, P. Dittanet, A. Seubsai, P. Prapainainar, *J. Phys.: Conf. Ser.* **2022**, *2175*, 012038.

[35] K. Mam, R. Dangtungee, *Mater. Today: Proc.* **2019**, *17*, 1914.

[36] K. Panploo, B. Chalermsinsuwan, S. Poompradub, *RSC Adv.* **2019**, *9*, 28916.

[37] E. K. Lee, S. Y. Choi, *Korean J. Chem. Eng.* **2007**, *24*, 1070.

[38] S. N. I. Kudori, H. Ismail, S. R. Khimi, *Mater. Today: Proc.* **2019**, *17*, 609.

[39] S. N. I. Kudori, H. Ismail, *Cell. Polym.* **2020**, *39*, 57.

[40] L. Lin, Z. Zheng, X. Li, S. Park, W. Zhang, G. Diao, Y. Piao, *Ind. Crops Prod.* **2023**, *192*, 116036.

[41] W. Zhang, L. Lin, L. Zhang, Y. Wang, Y. Zhuang, Y. Choi, Y. Cho, T. Chen, H. Yao, Y. Piao, *ACS Appl. Polym. Mater.* **2022**, *4*, 54.

[42] U. Narumitbowonkul, P. Keangin, P. Rattanadecho, *Int. J. Mech. Mechatronics Eng.* **2015**, *9*, 518.

[43] N. S. A. Zauzi, Z. M. Ariff, S. R. Khimi, *Mater. Today: Proc.* **2019**, *17*, 1001.

[44] K. Jitkokkruad, K. Jarukumjorn, C. Raksakulpiwat, S. Chaiwong, J. Rattanakaran, T. Trongsatitkul, *Polymers* **2023**, *15*, https://doi.org/10.3390/polym15030654.

[45] S. Chaiwong, R. Saengrayap, J. Rattanakaran, A. Chaithanarueang, S. Arwatchananukul, N. Aunsri, K. Tontiwattanakul, K. Jitkokkruad, H. Kitazawa, T. Trongsatitkul, *Postharvest Biol. Technol.* **2023**, *199*, 112273.

[46] A. Lopez-Gil, F. Silva-Bellucci, D. Velasco, M. Ardanuy, M. A. Rodriguez-Perez, *Ind. Crops Prod.* **2015**, *66*, 194.

[47] J. Pinto, E. Solórzano, M. A. Rodriguez-Perez, J. A. De Saja, *J. Cell. Plast.* **2013**, *49*, 555.

[48] ASTM D1621-00, Standard Test Method for Compressive Properties of Rigid Cellular Plastics, https://doi.org/10.1520/D1621-16R23.

[49] ISO 291:2005 Plastics — Standard Atmospheres for Conditioning and Testing, Geneva, Switzerland, **2005**, https://www.iso.org/standard/38242.html.

[50] S. Mundi, R. E. Aluko, *Food Res. Int.* **2012**, *48*, 299.

[51] I. Lassoued, M. Jridi, R. Nasri, A. Dammak, M. Hajji, M. Nasri, A. Barkia, *Food Hydrocoll.* **2014**, *41*, 309.

[52] D. Daugelaite, R. M. Guillermic, M. G. Scanlon, J. H. Page, *Colloids Surf., A* **2016**, *489*, 241.

[53] J. Asami, B. V. Quevedo, A. R. Santos, L. P. Giorno, D. Komatsu, E. A. de Rezende Duek, *Int. J. Biol. Macromol.* **2023**, *253*, 126782.

[54] G. Luciano, A. Vignali, M. Vignolo, R. Utzeri, F. Bertini, S. Iannace, *Materials* **2023**, *16*, https://doi.org/10.3390/ma16083063.

[55] A. Jones, M. A. Zeller, S. Sharma, *Prog. Biomater.* **2013**, *2*, 1.

[56] T. M. S. U. Gunathilake, Y. C. Ching, H. Uyama, D. H. Nguyen, C. H. Chuah, *Int. J. Biol. Macromol.* **2021**, *193*, 1522.

[57] E. J. Guidelli, A. P. Ramos, M. E. D. Zaniquelli, O. Baffa, *Spectrochim. Acta, Part A* **2011**, *82*, 140.

[58] N. T. Zapata-Gallego, M. L. Álvarez-Láinez, *J. Polym. Environ.* **2019**, *27*, 364.

[59] Y. Chen, J. Hu, X. Yi, B. Ding, W. Sun, F. Yan, S. Wei, Z. Li, *LWT* **2018**, *95*, 282.

[60] P. Li, Z. Sun, M. Ma, Y. Jin, L. Sheng, *LWT* **2018**, *97*, 151.

[61] Y. Zhu, S. K. Vanga, J. Wang, V. Raghavan, *Food Bioprocess Technol.* **2018**, *11*, 1974.